

Evaluate the Snow Depletion Curve Theory in the American River Basin with Distributed Snow Model

Eylon Shamir, Ph.D.
Post Doctoral Associate
Hydrologic Research Center
12780 High Bluff Drive, Suite 250
San Diego, CA 92130

Tel: 858-794-2726
Fax: 858-792-2519
Email: eshamir@hrc-lab.org
Web: www.hrc-web.org

BIOGRAPHICAL SKETCH

Since graduating from the University of Arizona's Hydrology and Water Resources Department in 2003, Dr. Shamir has worked as a post doctoral associate for the Hydrologic Research Center in San Diego, which is a public benefit non-profit organization. His research interests pertain to hydrology and hydrometeorology.

Evaluate the Snow Depletion Curve Theory in the American River basin with Distributed Snow Model

Eylon Shamir, and Konstantine P. Georgakakos

HYDROLOGIC RESEARCH CENTER

12780 High Bluff Drive, Suite 250, San Diego, CA 92130, Tel: +(858) 794-2726 +(858) 794-2397

Fax: +(858) 792-2519. E-mail: Eshamir@hrc-lab.org;

Abstract

In numerical hydrologic snow models the Snow Depletion Curve (SDC) is commonly used to explain spatial variability in the snow pack within the modeling elements. This curve relates the Snow Cover Area (SCA) to the current Snow Water Equivalent (SWE), which is a model derived variable. A primary assumption carried in the exploitation of such curves is that the accumulation and ablation processes that control the areal SWE distribution are mainly related to the physical properties (e.g., topography, land cover) and climatic signals (e.g., prevailing wind, mean monthly precipitation distribution) of a given basin. Since these basin properties are assumed stationary over the years with relatively small inter annual variability the derivation of a single representative SDC curve is feasible. We test the aforementioned assumption in the upper part (i.e., >1500 meter) of the three forks (i.e., North, Middle, and South) of the American River Basin. The NWS snow-17 model which accounts for the current energy and mass states of the pack, was developed in 1-km² grid cells to provide both the SCA and the SWE as model variables. The model parameters were spatially distributed to account for radiation variation resulting from land cover and aspect, and 6-hour point observed surface temperature and precipitation was interpolated based on climatologically derived lapse rate and mean annual distribution map (PRISM), respectively. The model derived SDC showed uniqueness of SDC in the upper three Forks, however, entail large inter-annual variability. We developed a procedure that estimate SDC in the beginning of the melting season that is based on Snow Course data which reduces the uncertainty of the snow variables (e.g., SWE and melt) resulted from the SDC.

1. Introduction

Process based snow accumulation and ablation models typically describe one-dimensional (vertical) energy and mass budget changes in the snow pack (e.g. Anderson, 1976; Jordan, 1991; Martinec et al., 1994; Tarboton and Luce, 1997). Application of these models on a basin scale requires association of the vertical snow pack model with the spatial heterogeneities of the snow accumulation and ablation processes. This is done by applying the model to either a relatively small homogeneous model element (i.e. in the context of a distributed model) (e.g. Blöschl et al., 1991; Wigmosta et al., 1994; Daly et al., 2000; Shamir and Georgakakos, 2005); or to large model elements with effective basin parameters and average input fluxes (i.e. in the context of a spatially lumped model) in conjunction with a diagnostic functional relationship between prognostic model

variables and spatial variability traits. The latter approach is favored in operational hydrology that estimates stream discharge. See for example, the intercomparison of snowmelt from models for runoff prediction in operational hydrology by the World Meteorological Organization (1986).

In basin-scale numerical modeling of snow properties, spatial variability is mainly accounted for during the melting processes while the accumulation processes are assumed uniform over each modeling element. The variability is commonly described using a snow depletion curve (SDC). The SDC describes the relationship between snow water equivalent (SWE) and snow cover area (SCA). In its simplest form and in discrete time, a snow depletion curve may be represented by the functional relationship:

$$SCA_i = f(SWE_{i-1}; \underline{\beta}) \quad (1)$$

where attention is focused on a certain area with partial snow cover during the melting season, SCA_i is the snow cover area at the end of the time interval $(i-1, i)$, SWE_{i-1} is the spatial average of the snow water equivalent over the entire area at the end of the time interval $(i-2, i-1)$, and $\underline{\beta}$ is the vector of the curve parameters. The associated mass conservation equation for time interval $(i-1, i)$ of duration Δt may be expressed as:

$$SWE_i = SWE_{i-1} + SCA_i(P_{i-1,i} - M_{i-1,i})\Delta t \quad (2)$$

where $(P_{i-1,i} - M_{i-1,i})$ is the net average snow influx rate (precipitation – melt) over the interval $(i-1, i)$ of duration Δt and over the area of consideration.

Combining Equations (1) and (2) yields:

$$SWE_i = SWE_{i-1} + f(SWE_{i-1}; \underline{\beta})(P_{i-1,i} - M_{i-1,i})\Delta t \quad (3)$$

from which, we deduce that the SDC is the rate of change of the SWE per unit change in net snow influx rate. It is apparent that: (1) changes in SWE depend significantly on the form and parameters of the SDC (function $f(\)$) during the melt season; (2) uncertainty in estimated SWE is significantly influenced by uncertainty in form and parameters of the SDC; and (3) past melt patterns within the area of consideration influence current melt patterns through dependence of the area depletion curve on past SWE and dependence of melt (M) on SWE.

A variety of SDC have been reported in the literature relating the SCA to a model simulated variable such as the cumulative production of snowmelt (Luce et al., 1999), and the current state of the SWE in the snow pack (e.g., Dunne and Leopard, 1978). The utilization of a characteristic SDC in snow models to account for the spatial variability within the modeling elements assumes that the accumulation and ablation processes are dominated by physiographic basin properties (e.g., topography, land cover) and prevailing local weather conditions. Therefore, the inter-annual accumulation and ablation processes are considered stationary with small annual variations and use of a

single curve that describes the relationship between the simulated snow variables and areal snow distributions is warranted.

However, because of the dependence of the validity of this assumption on the geographic location, various terrain features, and the scale of interest, analysis of the adequacy of using a single characteristic SDC for specific geomorphologic and hydroclimatic regimes is necessary. For instance, Mertinec (1980) reported that snow disappearance patterns are similar annually, though the snow cover area changes are dependent on the winter snow accumulations in the Swiss Alps. Such observation, lead to the development of family of SDC that are similar in shape, but with timing variations which depend on the initial SWE conditions.

In this study we examine the relationship between the SWE and the SCA in the steep terrain of the American River Basin. We, first, evaluate the adequacy and uncertainty associated with the use of a single SDC for prediction of snowmelt using a spatially lumped model, and, second, develop a procedure that estimates the SDC in the beginning of the melting season from ground snow survey data. The results are pertinent to real time flow prediction applications and to assessments of the potential influence of climatic changes on the timing and amount of melt in the study region.

We close this section with a review of pertinent literature to provide context for the analysis to follow. Description of the study area, methods, model and data is provided in Section 2. The results and discussion section (Section 3) is broken into model validation, analyses of the model derived SDC, uncertainty analyses of the SDC variability effects on spatially lumped modeling, and the development of a procedure for estimating the SDC in the beginning of the melt season based on snow course data. Last, we provide a summary of conclusions and recommendations for future research in Section 4.

1.1 Literature review

Derivation of the SDC requires several years of basin SWE and SCA observations at different times during the snow pack melting period. Efforts to derive such curves are reported for small experimental basins (e.g. Luce et al., 1999). However, such detailed datasets are unavailable in most locations. Lacking observations with high spatial resolution in larger basins necessitates the SWE estimation using interpolation and/or extrapolation techniques from existing gauge data (e.g. Elder et al., 1998; Chang and Li, 2000), while the SCA evolution can be estimated from areal photography (e.g., Martinec 1975) or remote sensing (e.g., Hall et al., 2002; Rosenthal and Dozier, 1996).

Methods to facilitate the derivation of the SDC that simplify and generalize spatial melting processes were reported. For instance, Liston (1999) formulated the relationship among the within-grid SWE distribution, gridcell melt rate during the season, and the within-grid depletion of SCA. Three methods of derivation of the SDC from knowledge of the SCA and SWE distributions at the end of winter were suggested by Ferguson (1984) and tested in a small well-instrumented watershed ($\sim 1 \text{ km}^2$) by Buttle

and McDonnell (1987). The different methods carry the following assumptions: (1) SWE is spatially uniform, and uniform melt occurs from the snow pack margins; (2) non-uniform SWE distribution prevails while the area decreases linearly with SWE content and the melt rate increases linearly with decreasing SWE; and (3) spatially varying SWE is associated with uniform melt. A more common approach proposed by Dunne and Leopold (1978) is to indicate the spatial variability of the SWE at the beginning of the melting season (i.e. at the peak SWE) and applying a uniform melting rate.

Some studies assign the SWE distribution at the end of winter a statistical distribution that corresponds to the specific basin. Examples include Luce et al, (1999) using a generic probability density function, and Manoes and Brubaker (2001) using a beta distribution. Studies also relate the statistical distribution parameters to the basin physical properties. Examples include Kolberg and Gottschalk (2003) that use a two-parameter Gamma distribution, and Donald et al. (1995) that use a log normal function parameterized based on land cover categories (i.e., short grass, ploughed fields or deciduous forest).

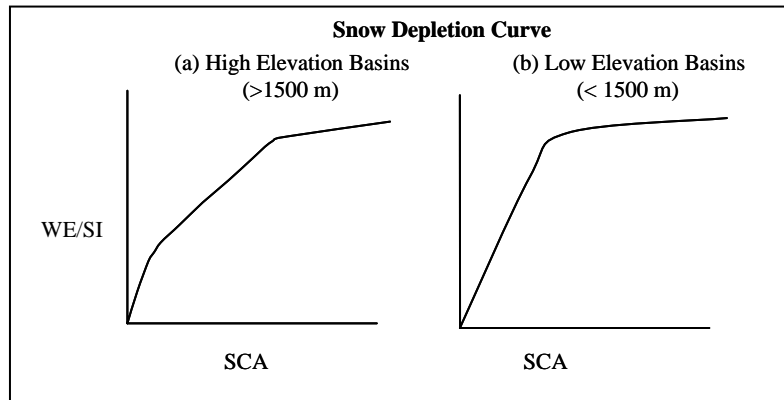


Figure 1. Conceptual estimates of typical SDC functions in the mountainous region of the Sierra-Nevada. The left panel (a) is for the SDC in the high elevation basins (above 1500 m), while the right panel (b) is for the SDC in low elevation basins (below 1500 m)

Most of the detailed validation studies referenced above were conducted in well instrumented small scale basins (O 0.1-10 km). However, in an operational setting that concerns larger basins (O 100 -10000 km²), typical SDC shapes are proposed as initial estimates which are later tuned to achieve an adequate fit between the simulated and observed downstream hydrographs (e.g., Anderson 1976). Fig. 1 shows examples of the SDC for high and low elevation basins in Sierra Nevada used as initial functional forms by the California Nevada River Forecast Center (CNRFC) of the National Weather Service (NWS) in conjunction with their operational spatially-lumped snow accumulation and ablation model. Generally, for high elevation basins (above 1500 m) such as for the American River headwater basins the curve of the left panel is used as an initial estimate for which a large snow mass ablates with rapid changes in snow cover area at the beginning and smaller changes at the end of the melt season. A rapid depletion followed by slow depletion of the SCA characterizes initial estimates of the SDC for the lower

elevation basins (below 1500 m) (Peter Fickenscher, CNRFC, personal communication). In the plots of Fig. 1, the SWE is divided by the normalizing parameter SI . SI is either the mean basin SWE since the beginning of snow accumulation, or a preset parameter of maximum SWE above which the areal extent is always 100%.

We note lastly the recent evidence of systematic changes in the hydrologic regime (e.g. Roos 1987; Cayan et al., 2001) and general agreement among the scientific community on future warming in the Sierra Nevada (e.g., Barnett et al., 2004; Dettinger et al., 2004). In this context, better understanding of the uncertainty in the snow model that is associated with parametric uncertainties is warranted. This is particularly important as adaptations of the NWS operational spatially-lumped snow accumulation and ablation model were used to assess the effect climate change scenarios have on the hydrological cycle and availability of water resources in the study region (e.g. Lettenmaier and Gan 1990; Carpenter and Georgakakos 2001; Yao and Georgakakos 2001; Miller et al., 2003). In these studies projections from future global climate model scenarios were downscaled to force basin hydrologic models and parameterized SDC functions were used.

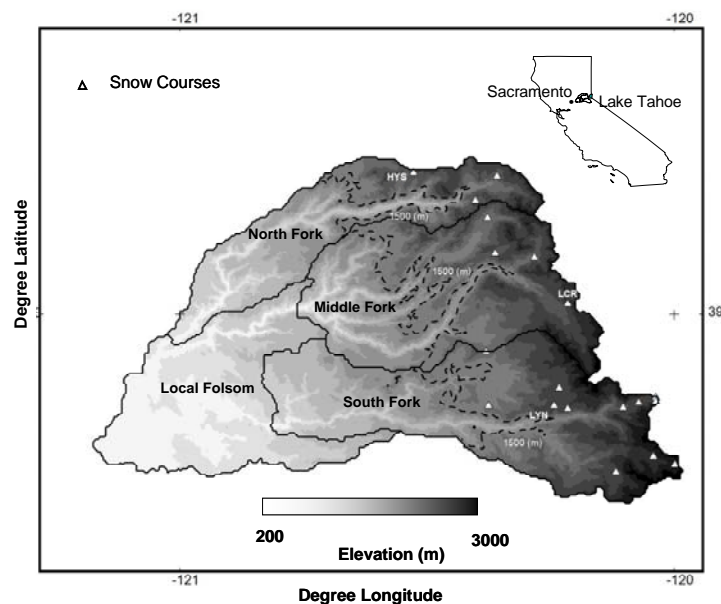


Figure 2. An elevation map of the American River Basin with the location of the snow courses indicated.

2. Data and methods

2.1 Study area

The study was conducted for basins of the American River, which flows westward from the crest of the Sierra Nevada and drains water into the Sacramento River (Fig. 2). We focus on a drainage area of about 4,740 km² which is above Folsom Lake

(longitude (121.2° - 119.9° and latitude 38.6° - 39.4°). The Folsom Lake Dam was constructed in the 50's to have a capacity of about 1200 10⁶ m³ (1- million acre-feet) for flood mitigation, water resources management and energy production. The Lake receives its natural flow from the North, Middle, and South Forks of the American River (Fig. 2). The Fork drainages are steep rocky canyons with fast water conveyance. The North Fork maintains natural flow as it drains a relatively unimpaired basin. Both the Middle and South Fork basins have regulated reservoirs and diversion canals.

Climate in this region is defined as Mediterranean, i.e., most precipitation occurs in the winter alternating between rainfall and snowfall, and the summers are generally dry and hot. Snowfall and temperature variability develop an intermittent winter snow pack in high elevations (typically above 1,500 meters) that melts completely during the spring and early summer. Prediction of the timing and magnitude of snowmelt is crucial for both long and short term Lake management considerations. The mean areal precipitation has large inter-annual variability and significant variability in the areal distribution with elevation (450 to 1800 mm year⁻¹).

2.2 Snow model description

We use an adaptation of the Anderson (1976) model, applied in a distributed manner within ~1-km grid cells, to derive estimates of the SDC. For a detailed description the model, the interested reader is referred to Anderson (1976). This model is constructed to account for the energy and mass balance of the snow pack. The snow model was developed to run in conjunction with a rainfall-runoff model. The model states are the energy deficit of the snow pack, an antecedent temperature index that approximates snow pack temperature, the liquid water equivalent of the snow pack, and the volume of the liquid water in the snow pack. Energy balance is controlled by the heat deficit, which allows refreezing of the available liquid water in the snow pack.

The model requires input data in the form of mean areal surface temperature (MAT) and cumulative mean areal precipitation (MAP). The MAT is used as an index to energy exchange across the snow-air interface. It is used to compute snow melt heat exchange and to determine snowfall from rain. During periods with no precipitation but warm temperatures, a seasonally varied melt factor is used to produce the volume of melt. During rain or snow events a simplified energy balance approach that considers temperature and precipitation data is used. The model also accounts for snow soil interface interaction, and liquid water storage. The vertical routing of the liquid water flow through the snow pack is not used in the model version adapted for this study.

The model elements consist of 1-km grid cells associated with the digital elevation model (DEM) acquired from GTOPO30, which is a global DEM dataset with ~1-km resolution, assembled by the US Geological Survey. CNRFC provided 6-hourly cumulative precipitation and instantaneous 6-hourly surface temperature data as MAP and MAT time series for seven American River basins for the period 1 October 1960 to 30 September 1999. Each of the three Fork basins was divided into an upper and a lower sub-basin and input time series were also provided for a local Folsom Lake sub-basin. These time series were generated from the standard quality-controlled gauge data using

standard NWSRFS interpolation procedures following the NWS manual calibration protocol.

The MAT and MAP time series were used to generate input for each distributed model gridcell. The surface temperature was distributed based on a diurnally varied lapse rate applied to the elevation differences from the elevation of the upper Middle Fork MAT series. In order to distribute the precipitation to the model gridcells, we used the PRISM (Parameter-elevation Regressions on Independent Slopes Model) map, which is a 2.5 arc min (~4km) mean annual precipitation (1961-1990) map created for the conterminous US (Daly et al., 1994). The precipitation values were distributed based on the proximity of the model element's center to the center of the PRISM gridcell. The precipitation time series was applied at the location where the average annual precipitation is 1500 mm year⁻¹, and the precipitation for the other model elements was distributed to maintain the same ratio of local to reference precipitation as observed from the PRISM map.

The melt factor, i.e. the factor of proportionality between melt rate and temperature, is varied annually by a sine function that is bounded with a priori estimated maximum and minimum melting factors valid on 21 June and 21 December, respectively. To implicitly account for some of the spatial variability of the incoming solar radiation, for the gridcells facing north (315° - 45°) these two parameter values were decreased by 20%, while for the gridcells facing south (135° - 225°) they were increased by 20%. For the remaining terrain aspects, the minimum and maximum melt factor values are set to 0.55 and 0.9 (mm °C 6hr⁻¹), respectively. The values of the remaining model parameters were taken from the CNRFC operational parametric database and are presented in Table 1. For a more detailed description of the distributed snow model, the reader is referred to Shamir and Georgakakos (2005).

Table 1. Snow model parameters and values.

<i>Parameter</i>	<i>Value</i>
SCF - Snow Correction Factor	1.05
MFMAX - Maximum Melt Factor during non rain periods (mm C° 6hr ⁻¹) in western facing slope	1.05
MFMIN - Minimum Melt Factor during non rain periods (mm C° 6hr ⁻¹) in western facing slope	0.6
UADJ – Average Wind Function during Rain on Snow (mm/mb)	0.04
NMF – Negative Melt Factor (mm _e C° ⁻¹)	0.15
TIPM – Antecedent weight factor	0.25
PXTEMP - determination of rain from Snow (C°)	2
MBASE – base temperature C°	1
PLWHC –Percent Liquid Water Holding Capacity	0.04
DAYGM – Snow Soil Interface Melt Factor (mm day ⁻¹)	0.3
Daily Maximum Lapse Rate (°C 100 m ⁻¹)	0.8
Daily Minimum Lapse Rate (°C 100 m ⁻¹)	0.45
Adjusted Elevation (meter)	2264
Adjusted Annual Mean Areal Precipitation (mm)	1500

3. Results and discussion

3.1 Model validation

A comprehensive evaluation of the distributed snow model was conducted during the water years 2000 -2004 and is discussed in detail in Shamir and Georgakakos (2005). For these years the model evaluation was compared to both SCA and SWE observations. The simulated SCA was compared during cloud free days to the MODIS (Moderate Resolution Imaging Spectroradiometer carried on the Terra satellite) 500m daily areal snow extent product (MOD10A1 version 4) (Hall et al., 2000). In Fig. 3 we show sample results of model and MODIS SCA comparisons for 17 March and 6 April 2003. These two snapshots that represent the beginning of and a time in the melt season, respectively, show good agreement in the SCA areal distribution. The main validation conclusion reported in Shamir and Georgakakos (2005) for the 2000-2003, using the same modeling scheme, is that both the SWE and the SCA were simulated well for the 6-hour and 1-km scales. The results of the validation showed that the distributed model replicates well the terrain features and the snow distribution areas. Model improvement is needed in the simulation of snow at the transition elevations in which the precipitation events are mixed rain and snow and at the lower boundaries of the snow pack.

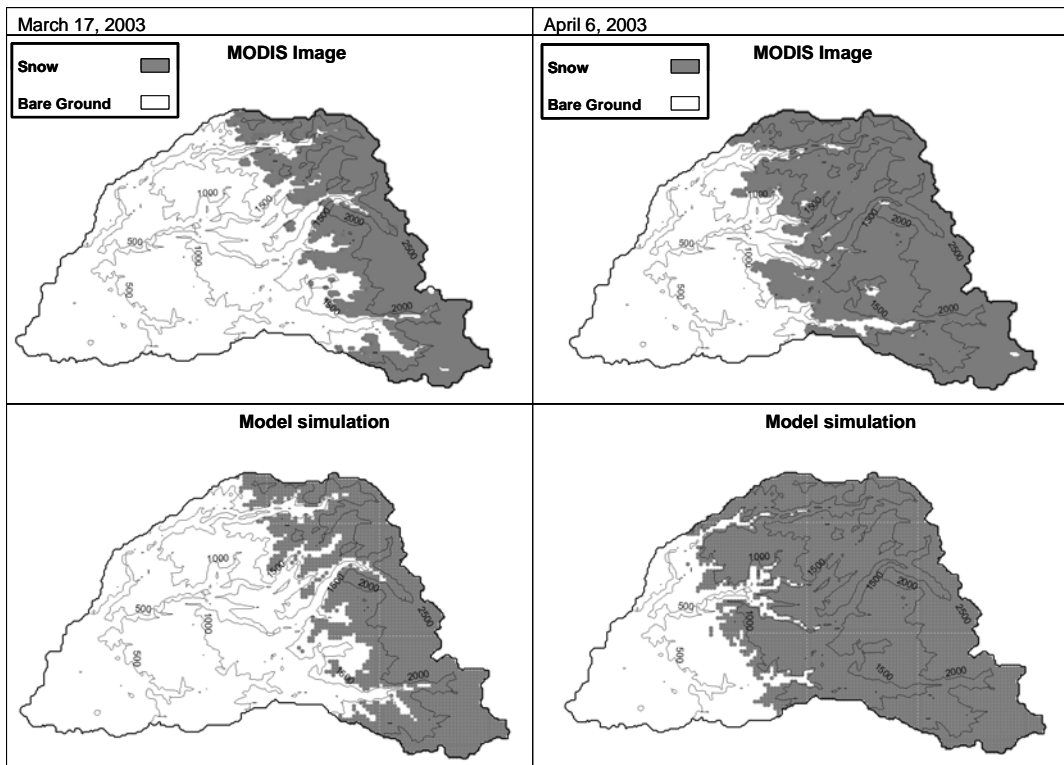


Figure 3. A comparison between the SCA from the MODIS daily 500 meter product and the model simulation for 17 March (left panels) and 6 April (right panels) of 2003.

Clearly such comprehensive validation of the SCA simulation with satellite spectral data is not feasible for the historical period 1960-1999. However, in Fig. 4 we present a comparison of SWE data from 20 snow courses in various locations in the basin (Fig. 2) to the daily model simulations of the corresponding gridcell. The comparison is done with all the snow course data available for the water years 1990-1999. We used unadjusted survey data that was acquired from the California Data Exchange Center (<http://cdec.water.ca.gov>).

The snow courses are survey data that are collected at the beginning of the month from January through April, and May to June in some years. Fig. 4 shows that all the comparisons produced apparent functional relationships that indicate good agreement between the observations and simulations. The correlation coefficient, R , shown in the Figure is higher than 0.77. In general, the higher elevations exhibit better agreement between the snow course data and the simulations on the gridcell scale.

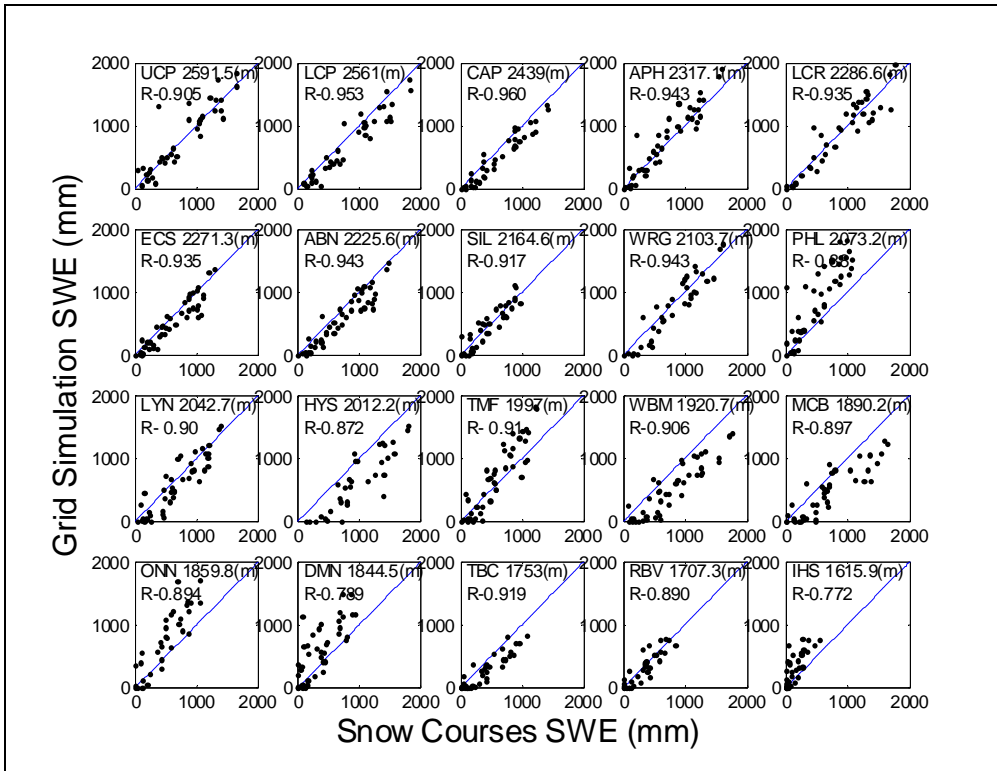


Figure 4. Comparison between the SWE from snow courses and from the model simulation for the corresponding grid. The comparison is for the period 1990-1999.

3.2 Estimation of the SDC

The distributed model simulation provides information on SWE for a single gridcell. By defining a gridcell with $SWE > 20\text{mm}$ as snow covered, the basin SCA can be estimated. Thus, the SDC can be computed from these model variables as indicated in

Eq. (1). We derive the annual SDC for the simulated years for the three upper Forks of the American River (areas with elevations higher than 1,500 meters). The beginning of the melting season was defined as the time of the maximum SWE value over all the gridcells in the basin that occurred after February. The raw computed points of the SDC curves were used to produce monotonic curves. This use of a single total maximum SWE as an indicator for the beginning of the melt season in the basin of interest implies that the melt season starts in all the basin gridcells at the same time. This assumption appears reasonable based on preliminary numerical experiments that show that during the melt season melting occurs over the entire basin although it varies in rate.

The model derived SDC for the upper part of the Forks are presented in Fig. 5 for each year of record. Main inferences are that: (1) the estimated SDC functions in all the Forks have large inter-annual variability; and (2) the shape of the curve estimated for the North Fork is seemingly different than that estimated for the Middle and South Forks, especially for low SWE values.

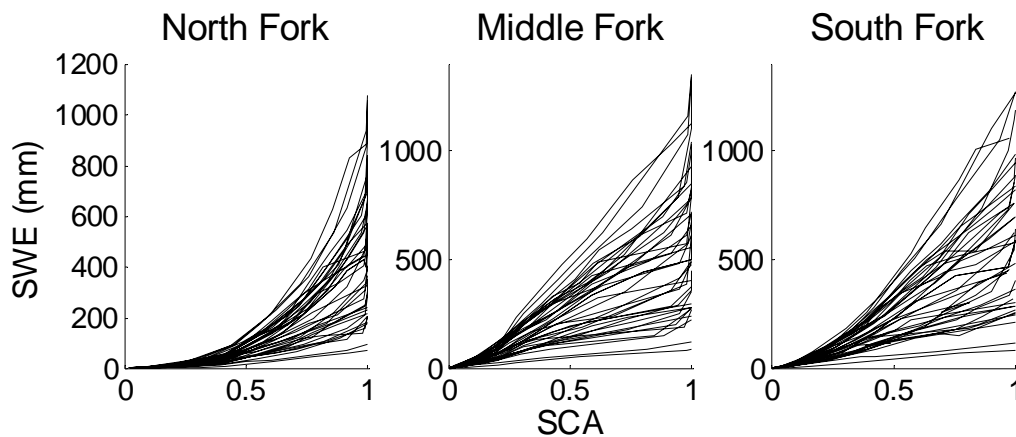


Figure 5. Snow depletion curves derived for the upper American River Forks (elevations higher than 1,500 meters) from the distributed model simulation and for the water years of 1960-1989.

3.3 SWE and melt uncertainty associated with the SDC variability

To assess the inter-annual variability impact of the SDC on the simulation of SWE, in Fig. 6 we plot 37 traces of SWE generated using forcing from the water year (1999-2000) in the upper North Fork. This year (1999-2000) was not included in the historical years with data used for the derivation of the SDC. Each trace was generated from the derived SDC of the upper North Fork. The SDC curves were normalized by the value of the simulated annual minimum SWE for which the SCA is 1. In spatially lumped procedures this parameter is the minimum value of a priori estimated static parameter or the maximum SWE of the current winter season up to the present. Such an approach, assumes consistency over the years in the relationships between the SWE and

the SCA. The distributed model derived SI values have a large variability that ranges from about 70 and 90 to 1000, 1250 and 1270 (mm) of SWE for the North, Middle and South Forks, respectively.

It can be seen in Fig. 6 that the effect of the SDC variability is magnified with the progression of the melting season, and the rate of melt and the depletion of the pack are highly sensitive to the SDC. The annual values of the coefficient of variation of the daily SWE estimated by the different SDC functions, shown in the middle panel of the Figure, increases monotonically with the progression of the melting season. This increase in time is because of the time dependence of the SDC as shown in Eqs. (1) and (2). Observing the effect of such SDC variation on the cumulative rain plus melt curve (lower panel in Fig. 6) indicates that the resultant outflow variability occurs mainly during the melt season with a small effect on the total annual RAIM.

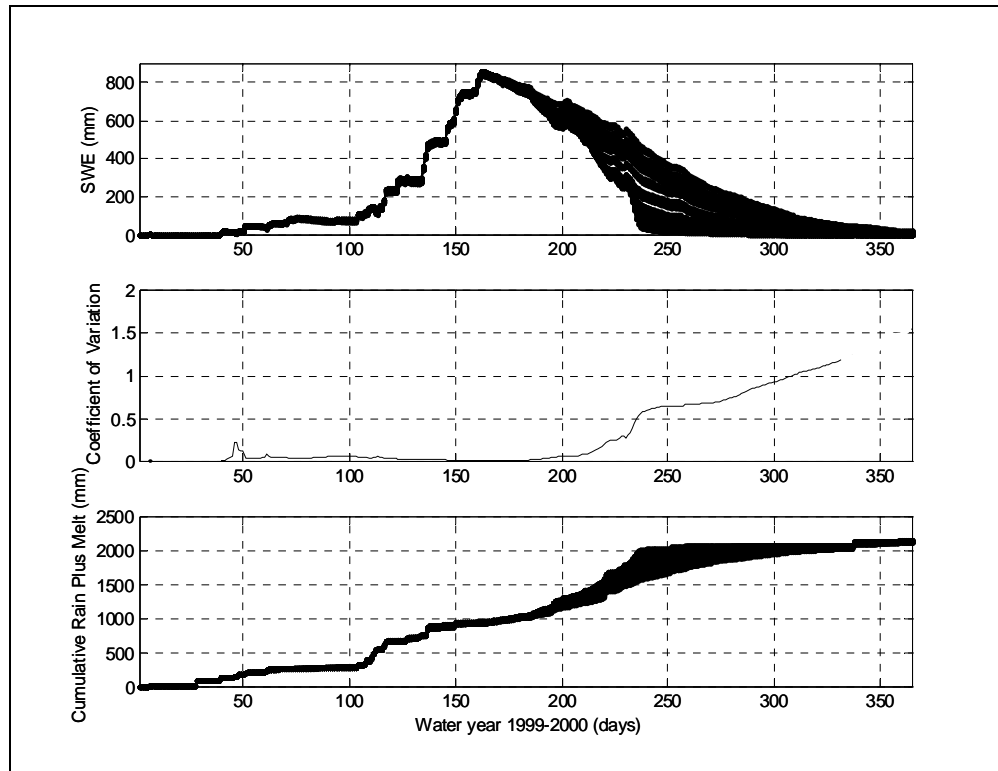


Figure 6. Spatially lumped simulation of the Upper North Fork mean basin SWE (mm) (upper panel) and cumulative basin rain-plus-melt (mm) (lower panel) resulting from the 1999-2000 water year forcing and using the derived SDC estimates from 1960-1989.

These numerical experiments reveal that the use of a single characteristic SDC in spatially lumped modeling procedures introduces large uncertainty, mainly in the timing and variability of the melt season flows. There is large inter-annual variability in the value of the minimum SWE that maintains complete snow cover. Reducing the uncertainties of spatially lumped models arising from the utilization of a single SDC function requires that the SDC is estimated annually in a predictive mode. In the next

section we analyze the SDC functions from the numerical experiments and derive empirical relationships that can be utilized for future applications of SDC annual prediction.

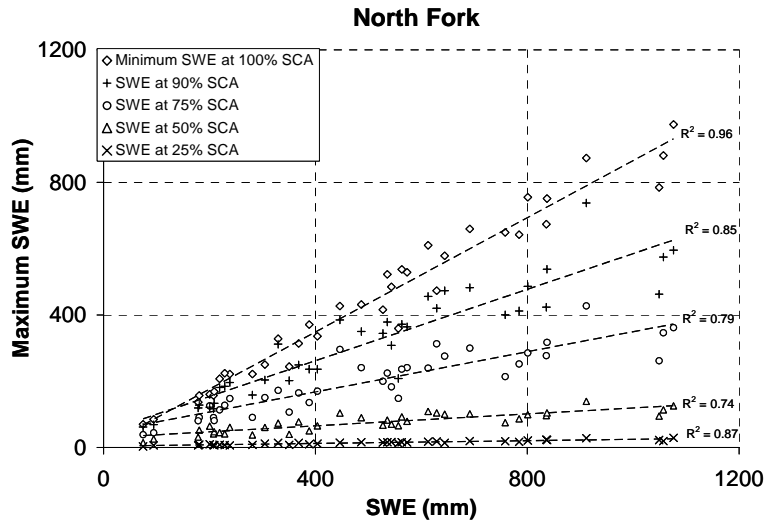


Figure 7. The simulated upper North Fork 1960-1989 relationships between the maximum seasonal SWE and the minimum SWE that maintained 100% SCA, and the SWE at 90%, 75%, 50% and 25%.

3.4 Empirical procedure to derive SDC from snow courses

Dependence of the SWE on the maximum SWE value of the winter season is assessed in the following for the melt season. In Figs. 7, 8 and 9 the SWE at 25 50 75 and 90% snow cover are plotted as a function of the maximum value for the North, Middle and South Fork, respectively. In addition, the minimum SWE that maintains 100% snow cover is also plotted in these Figures.

It is seen for all the Forks that the SWE and the SCA at the progression of the melt season is strongly related to the maximum SWE at the beginning of the season. In other words, years that show high maximum SWE values in the beginning of the season would show high SWE values later in the season for the different SCA stages and vice-versa. It can be seen that these correlations are weaker for the low SCA values but arguably still significant (the lowest correlation coefficient is 0.71 at the South Fork). Such results also imply that for the study region the *SI* should in practice be selected as the maximum SWE that occurred to date, which seem to correspond well with the presented analysis.

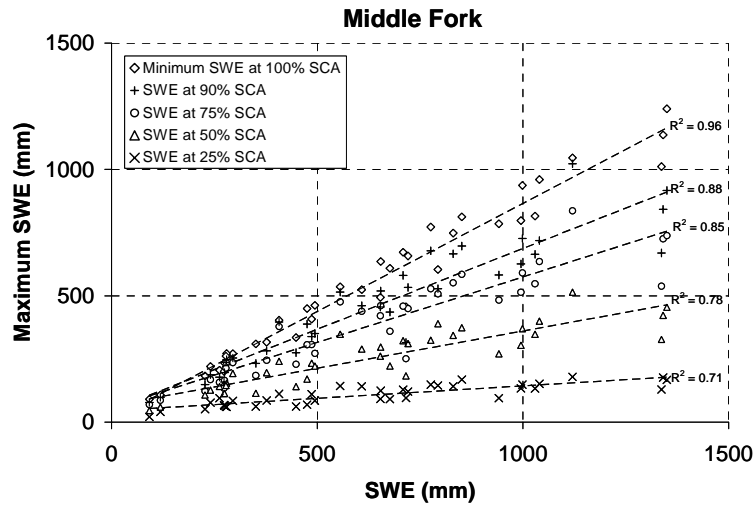


Figure 8. The simulated upper Middle Fork 1960-1989 relationships between the maximum seasonal SWE and the minimum SWE that maintained 100% SCA, and the SWE at 90%, 75%, 50% and 25%.

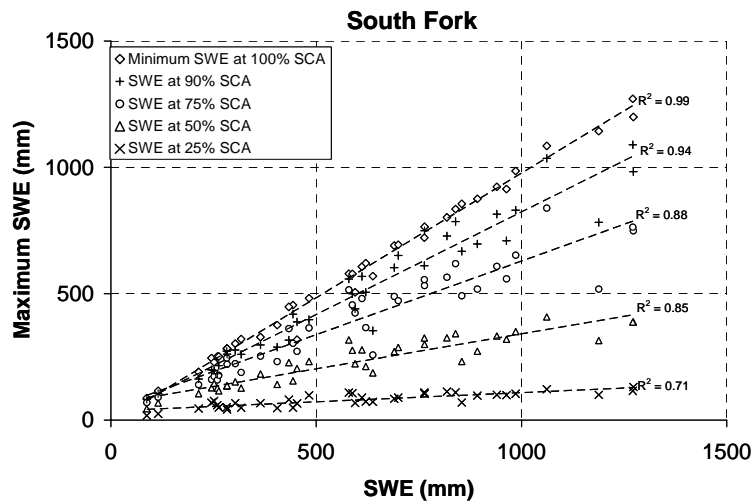


Figure 9. The simulated upper South Fork 1960-1989 relationships between the maximum seasonal SWE and the minimum SWE that maintained 100% SCA, and the SWE at 90%, 75%, 50% and 25%.

Although these results might seem as a quantitative confirmation of an intuitive assumption, they carry potential use for a predictive utilization of the SDC. If one can quantify the SWE at the beginning of the melt season, an estimate of the SDC can be derived from the above relations using simple regression equations. The prediction of the SWE at the beginning of the melt season can potentially be related to observations from

surveys (snow courses). In this study we selected the beginning of March as an index for the maximum SWE that occurred during the season.

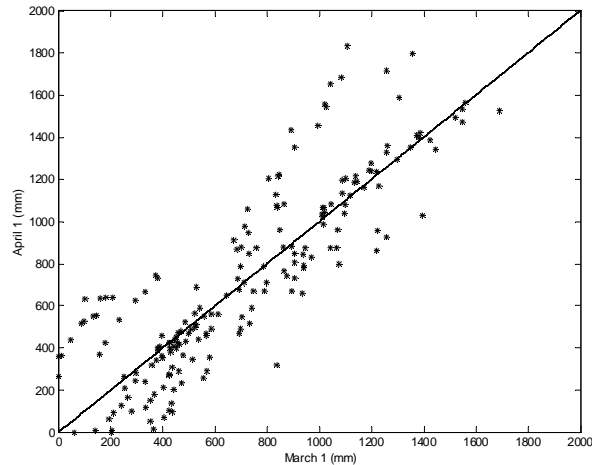


Figure 10. A comparison between SWE at the beginning of March versus the beginning of April from 20 snow courses in the American River for the period 1990-1999

In Fig. 10 we show a comparison for 1990-1999 that shows the 20 courses on the American River survey of March and April. It may be seen that both survey dates can be equally considered as an index for the maximum SWE occurrence. However, the selection of the March survey provides a longer lead time for the estimation of the SDC within the melt season.

The HYY, LCR and LYN snow course locations were selected to represent the North, Middle and South Forks, respectively (Fig. 1). In Fig. 11, the course and the maximum SWE are plotted. Clearly, there exists a linear relationship with correlation coefficients of 0.79, 0.79 and 0.74 for the North, Middle and South Forks, respectively. These coefficients were computed with the exclusion of the few marked outliers.

The linear relationships between the model maximum SWE and the SWE for a given SCA (Figs. 7, 8 and 9), and the later linear relationship between the maximum SWE and the course survey data at the beginning of March, potentially provide a simple method to derive the SDC at beginning of the season in a predictive mode. In Table 2 the slope (a) and the y-axis intercept (b) parameters of these linear regressions are provided.

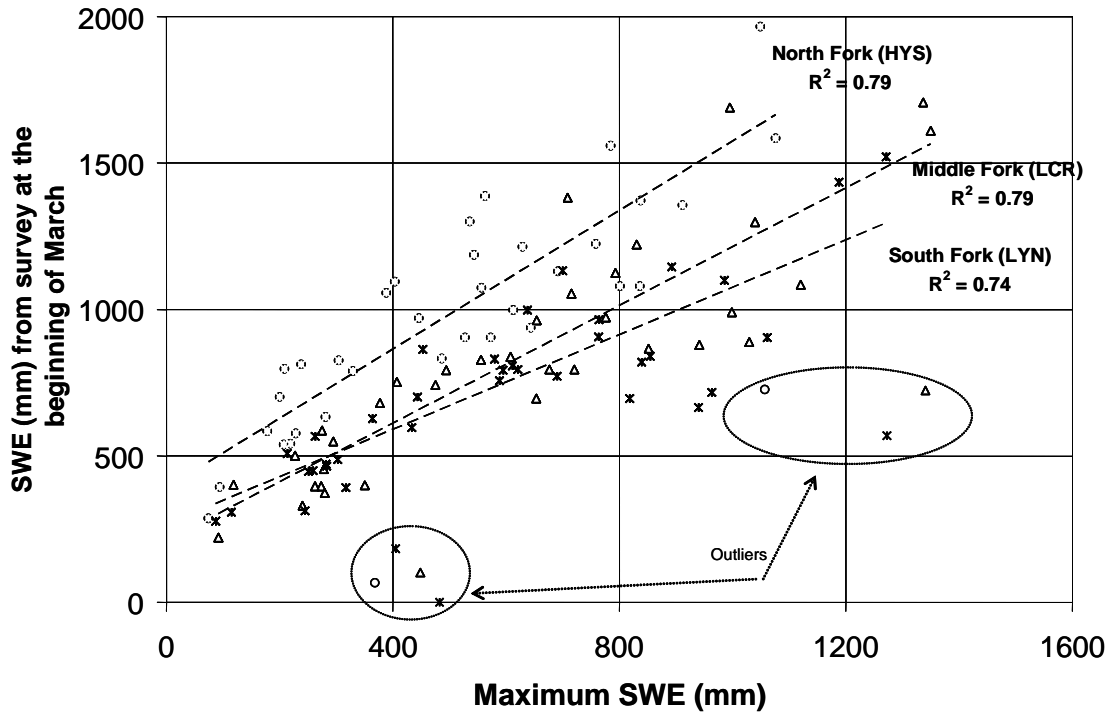


Figure 11. Three snow courses, Hysink (HYS), Lower Canyon Mountain (LCR) and Lyons Creek (LYN) SWE at the beginning of March for 1960-1989 as functions of the maximum basin SWE simulated for the 1960-1989 period in the three upper American River Forks,

4. Conclusions and recommendations

In this study we evaluated the validity of the assumption that there is a static annual relationship between the SWE and the SCA during the melting season described by a characteristic snow depletion curve (SDC). The study was conducted by deriving these relationships explicitly using prognostic distributed snow model output for the basins of the three upper Forks of the American River for the water years 1960-1999. The model estimated SDC functions share a unique shape that characterizes the different Forks; however the SDC inter-annual variability is large. The effect of such variability is demonstrated and found to largely impact the timing of the snow melt. As such, one must exercise caution when assessing the timing of snow melt with spatially lumped models in real time or longer term predictions (e.g. associated with climate change scenarios).

Analysis of the model derived SDC indicates that the SWE for a given SCA is related to the maximum SWE of the year at the end of the winter. Moreover, this maximum SWE is found to be correlated with early March snow course data from the corresponding Fork basin. Such results provide a simple procedure to adjust the SDC curve at the beginning of the melt season. This procedure could potentially reduce the uncertainty in the snow melt estimates.

In future studies the idea presented here should be validated to confirm these reported relationships using different model setups. For example, using models with different temporal and spatial scales and using dynamical downscaling methods to distribute the model meteorological input onto the model elements. Application to areas in different hydroclimatic regimes is also a natural extension of this work.

Table 2. Linear regression parameters that relate the basin SWE at a given SCA fraction as a function of the annual maximum SWE, and the estimate of the annual maximum SWE as a function of the snow course SWE observations. Parameter a is the slope and parameter b is the intercept with the y-axis

	<i>North Fork</i>		<i>Middle Fork</i>		<i>South Fork</i>	
	<i>a</i>	<i>b</i>	<i>a</i>	<i>b</i>	<i>a</i>	<i>b</i>
SI	0.86	3.3	0.86	10.5	0.99	-8.6
90% SCA	0.54	45.8	0.64	47.4	0.81	11.6
75% SCA	0.30	46.3	0.52	56.1	0.58	46.6
50% SCA	0.09	28.8	0.29	65.7	0.28	64.1
25% SCA	0.02	3.4	0.10	44.7	0.07	35.6
<i>Snow Courses</i>	<i>HYS</i>		<i>LCR</i>		<i>LYN</i>	
Max SWE	1.18	391.4	1.0	210.6	0.81	266.7

Acknowledgements

We wish to express our gratitude to the CNRFC personnel, especially to Peter Fickenscher, Eric Strem, and Robert Hartman, for providing data and technical support. This research was done as part of the INFORM Project, sponsored by the National Oceanic and Atmospheric Administration, the California Energy Commission and the CALFED Bay Delta Authority. The ideas and opinions expressed herein are those of the authors and need not necessarily represent those of the sponsoring agencies and their sub-agencies.

References

- Anderson, E.-A., 1976. A point energy and mass balance model of a snow cover. Silver Spring, MD US. National Oceanic and Atmospheric Administration (NOAA) Technical Report NWS 19.
- Barnett, T., Malone, R., Pennell, W., Stammer, D., Washington, W., 2004. The effects of climate change on water resources in the west: Introduction and overview. *Clim. Change*, 62, 1-11.
- Buttle, J.-M., McDonnell, J.-J., 1987. Modeling the areal depletion of snow cover in the forested catchment. *J. Hydrol.* 90, 43-60.

- Blöschl, G., Gutknecht, D., Kirnbaur, R., 1991. Distributed snow melt simulation in an alpine catchment, 2, Parameter study and model predictions. *Water Resour. Res.* 27, 3181-3188.
- Carpenter, T.-M., Georgakakos, K.-P., 2001. Assessment of Folsom Lake response to historical and potential future climate scenarios, 1. Forecasting. *J. Hydrol.* 249, 148-175.
- Cayan, R.-D., Kammerdiener, S.-A., Dettinger, M.-D., Caprio, J.-M., Peterson, D.-H., 2001. Changes in the onset of spring in the Western United States. *Bull. Amer. Meteor. Soc.* 82(3), 399-414.
- Chang K.-T., Li, Z., 2000. Modeling snow accumulation with a geographic information system. *Int. J. Geogr. Inf. Syst.* 14(7), 693-707.
- Daly, C.-R., Neilson, P., Phillips, D.-L., 1994. A statistical-topographic model for mapping climatological precipitation over mountainous terrain. *J. Appl. Meteor.* 33, 140-158.
- Daly, S.-F., Davis, R.-E., Ochs, E., Pangburn, T., 2000. An approach to spatially distributed snow modeling of the Sacramento and San Joaquin basins, California. *Hydrol. Processes* 14, 3257-3271.
- Dettinger, M.-D., Cayan, D.-R., Meyer, M.-K., Jeton, J.-E., 2004. Simulated hydrologic responses to climate variations and change in the Merced Carson, and American River basins, Sierra Nevada, California, 1900-2099. *Clim. Change*, 62, 283-317.
- Donald, J.-R., Soulis, E.-D., Kouwen, N., Pietroniro, A., 1995. A land cover - based snow cover representation for distributed hydrologic models. *Water Resour. Res.* 31(4), 995-1009.
- Dunne, T., Leopold, L.-B., 1978. *Water in Environmental Planning*. W. H. Freeman and Company, San Francisco.
- Elder, K., Rosenthal, W., Davis, R., 1998. Estimating the spatial distribution of snow water equivalence in montane watershed. *Hydrol. Proces.* 12, 1793-1809
- Ferguson, R.-J., 1984. Magnitude and modeling of snowmelt runoff in the Cairngorm mountains, Scotland. *Hydrol. Sci. J.* 29, 49-62.
- Jordan, R.-A., 1991. One dimensional temperature model for snow cover. *Spec. Rep. 91-6*, U.S. Army Cold Regions Res. and Eng. Lab, Hanover, N. H.
- Hall, D.-K., Riggs, G.-A., Salomonson, V.-V., 2000. MODIS/Terra Snow Cover 8-day L3 Global 500 m Grid V004, January 2003. Boulder, CO, USA: National Snow and Ice Data Center. Digital media.
- Hall, D.-K., Riggs, G.-A., Salomonson, V.-V., DiGirolamo, N.-E., Bayr, K.-J., 2002. MODIS snow-cover products. *Remote Sens. Environ.* 83, 181-194.
- Kolberg, S.-A., Gottschalk, L., 2003. Updating of Snow Depletion Curve with Remote sensing Data. EGS - AGU - EUG Joint Assembly, Nice, France 6-11 April 2003
- Lettenmaier, D.-P., Gan, T.-Y., 1990. Hydrologic sensitivities of the Sacramento-San Joaquin River Basin to global warming. *Water Resour. Res.* 26(1), 69-86.
- Luce C.-H., Tarboton, D.-G., Cooley, K.-R., 1999. Sub-grid parameterization of snow distribution for an energy and mass balance snow cover model. *Hydrol. Proces.* 13, 1921-1933.
- Liston E.-G., 1999. Interrelationships among snow distribution, snowmelt, and snow cover depletion: Implication for atmospheric, hydrologic, and ecologic modeling. *J. Appl. Meteor.* 38(10), 1474-1487.

- Manoes, M.-C., Brubaker, K.-L., 2001. How similar are snow depletion curves from year to year? Case study in the upper Rio Grande Watershed. 58th Eastern Snow Conference Ottawa, Ontario, Canada.
- Martinec J., 1975. Snowmelt–runoff model for streamflow forecast. *Nord. Hydrol.* 6(3), 145-154.
- Martinec J., 1980. Limitations in hydrological interpretations of the snow coverage. *Nord. Hydrol.* 11, 209-220.
- Martinec, J., Rango, A.-M., Roberts, R., 1994. The snowmelt-runoff model (SRM). User's Manual (ed. by Baumgartner) University of Bern, Switzerland.
- Miller, N.-L., Bashford, K.-E., Strem, E., 2003. Potential impacts of climatic change on California hydrology. *J Amer. Water Resources Assoc.* 39, 771-784.
- National Research Council. 1995. Flood Risk Management and the American River Basin, an evaluation. National Academy Press. Washington, D.C.
- Roos, M., 1987. Possible changes in California snowmelt runoff patterns. Proc. 4th Annual PACLIM Workshop, Pacific Grove, CA, 22-31.
- Rosenthal, W., Dozier, J., 1996. Automated mapping of mountain snow cover at subpixel resolution from the Landsat Thematic Mapper. *Water Resour. Res.* 32, 115-130.
- Shamir, E., Georgakakos, K.-P. 2005. Distributed snow accumulation and ablation modeling in the American River Basin. *Adv. Water Resour.* (in Review)
- Tarboton D.-G., Luce, M.-S., 1997. Utah Energy Balance Snow Accumulation and melt model (UEB). Computer model technical description and users guide. Utah Water Research Laboratory, Logan, Utah.
- Wigmosta M.-S., Vail, L.-W., Lettenmaier, D.-P., 1994. A distributed hydrology-vegetation model for complex terrain. *Water Resour. Res.* 30(6), 1665-1679.
- World Meteorological Organization, 1986. Intercomparison of models of snowmelt runoff, *Oper. Hydrol. Rep.* 23, WMO Publ. 646, Geneva, Switzerland.
- Yao, H., Georgakakos, A., 2001. Assessment of Folsom Lake response to historical and potential future climate scenarios. *J. Hydrol.* 249, 176-196.